Generation of Twisted Photons in the mm Wavelength Region and Investigation of its Properties

Srinidhi Rajagopalan

Supervisor: Dr Pavel Karataev

Department of Physics

Royal Holloway, University of London

PH4100 - Major Project Report

March, 2019

Abstract

Orbital angular momentum of light ('Twisted Photons'), is a fairly less understood feature of light compared to its sibling, spin angular momentum. This essay describes the procedure involved in the generation of the first order of orbital angular momentum in the mm wavelength region using a spiral phase plate in a Michelson interferometer and collecting observational data using a terahertz imaging sensor. This was achieved by the super-position of a Gaussian and a Laguerre-Gaussian beam in the Michelson interferometer built on the principles of Fourier-transform spectroscopy. The obtained superimposed beam with orbital angular momentum was verified theoretically in a python environment. Since orbital angular momentum of light is a relatively under explored feature of light, and its presentation has not been simplified yet, this report has also attempted to present a brief straightforward way to understand the complex characteristics of orbital angular momentum from research previously carried out while limiting to only the core aspects of it.

Contents

Chapter 1

Introduction

1.1 History

In the historical paper, "A Dynamical Theory of Electromagnetic Field" published by James Clerk Maxwell in 1865, he demonstrated the *wave nature of light*, where the electric and magnetic fields propagate with the speed of light [1]. This would mean that, electromagnetic radiation has both *energy and momentum.* Johannes Keppler suggested that the tail of a comet points away from the sun because of the *linear momentum* of light. Following his pursuit, in 1909, John Henry Poynting published a paper, based on the outcome, of a suspended section of a circular shaft which transmitted uniform power, parallel to the axis of the shaft, based on which he suggested that circularly polarized light has *angular momentum* (which was later recognized as spin angular momentum) [2]. He also established that the ratio of linear momentum to angular momentum is $\lambda/2\pi$ (whereλ is the wavelength of light). The idea was reinforced by Albert Einstein, who pointed out that the energy quanta must carry a momentum, $p = h\lambda$ (where, h is Planck's constant), as a consequence of Planck's law of black body radiation [3]. This momentum of a photon was observed in Compton scattering for which Arthur Compton received the Nobel Prize in 1927 [4].

In 1936, Richard A. Beth from Princeton University established methods for the detection and determination of spin angular momentum of light, using quartz wave plates [5]. Nobel Prize laureate, Dr. Arthur Ashkin recorded the first observation of

freely suspended particles being accelerated by the forces of radiation pressure (that is, When light is absorbed or reflected from a surface, there is an exchange of momentum between the surface and the electromagnetic radiation which consequently, exerts a pressure on the surface called as 'Radiation Pressure'.) from continuous wave, visible laser light. This paved the way to the discovery of stable 'Optical Wells' which trapped particles solely by the effect of radiation pressure [6].

Later, in 1992 L. Allen and his co-workers made the remarkable discovery that circularly polarized light also carries a well-defined orbital angular momentum (OAM) [7]. Prior to which, orbital angular momentum was only observed in higher order atomic or molecular transitions, which seldom occur in nature. His paper, also proposed a method for the measurement of mechanical torque induced due to the transfer of orbital angular momentum of light during the transformation of a Laguerre-Gaussian mode into a higher order Hermite Gaussian mode in an astigmatic optical system (that is, a system in which light rays having different foci, propagate perpendicular to each other). This was achieved by comparing the results from measuring the rotation of a fiber suspension and creating two opposing Laguerre-Gaussian modes, which was achieved by suspending two cylindrical lenses. These brilliant discoveries became the invaluable foundation over which further exploration over the extraordinary abilities of orbital angular momentum of light continues till day.

1.2 Motivation

The motive to pursue the project arose from four foundational reasons. The works of Nobel laureate Dr. Arthur Ashkin in 'Optical tweezers and their applications to biological systems' explores the capabilities of orbital angular momentum in the real world. It proved to show remarkable potential in its applications and that became the first source of inspiration. Secondly, the orbital angular momentum of light is a less explored feature of light which sets ground to study and observe new and exciting outcomes. Thirdly, it requires to work with various mechanical systems like a Michelson's Interferometer, a setup that is considered effective but widely known for its sensitive arrangement and modern equipment like THz camera which played a pivotal role in enabling one to observe orbital angular momentum of light with ease.This displayed a challenge which would provide incomparable experience and skill with optical systems. And lastly, but most importantly, the orbital angular momentum of light has not been observed in the mm wavelength region, which is a fairly, much longer wavelength region compared to the ones previously produced in the nm wavelength region. These reasons set the primal foundation to work on optical tweezers.

Chapter 2

Theory

2.1 Angular Momentum of Light

A beam of circularly polarized light, whose electric and magnetic fields rotate in a loop, continuously about the axis of propagation attributes to a vector quantity called *'Angular Momentum of Light'*. A light beam whose component fields rotate about its propogation axis carry two kinds of angular momentum: Orbital Angular Momentum (OAM) and Spin Angular Momentum (SAM) [8]. A circularly polarized light has an intrinsic property in the electromagnetic field called Spin Angular Momentum (SAM). A photon which is circularly polarized carries a SAM of $\pm\hbar$, where $\hbar$ is reduced Planck's constant. SAM is positive when the light beam is right polarized and it is negative when the light beam is left polarized with respect to the propagation axis. Orbital angular momentum arises due to the structure of the wavefront. The total angular momentum disregarding the two types of angular momentum is represented as follows.

$$\vec{J} = \epsilon_0 \int \vec{r} \times (\vec{E} \times \vec{B}) d^3\vec{r} \tag{2.1}$$

Where $\vec{J}$ is total angular momentum, ϵ_0 is the relativity of free space, $\vec{r}$ is the position vector, $\vec{E}$ is the electric field vector, $\vec{B}$ is the magnetic field vector. The total angular momentum inclusive of the radiation field is given by the summation of SAM and OAM

is represented as follows.

$$\vec{J}_{rad} = \vec{S}_{rad} + \vec{L}_{rad} = \left[\epsilon_0 \int d\vec{r}\vec{E}_{\perp} \times \vec{A}_{\perp}\right] + \left[\epsilon_0 \sum_l \int d\vec{r}\vec{E}_l^{\perp}(\vec{r} \times \nabla)\vec{A}_l^{\perp}\right] \quad (2.2)$$

Where, $\perp$ repersents the transverse portion of the optical field, $\vec{S}_{rad}$ is the transvere portion of spin angular momentum, $\vec{L}_{rad}$ is the transverse portion of orbital angular momentum, $\vec{A}_l^{\perp}$ is vector potential which is used instead of $\vec{E}$ and l is the azimuthal state associated with OAM. Eqn (2.2) is gauge invariant to ensure rotational invariance using Noether's theorem. Figure(2.1) illustrates a the difference in the structure of a

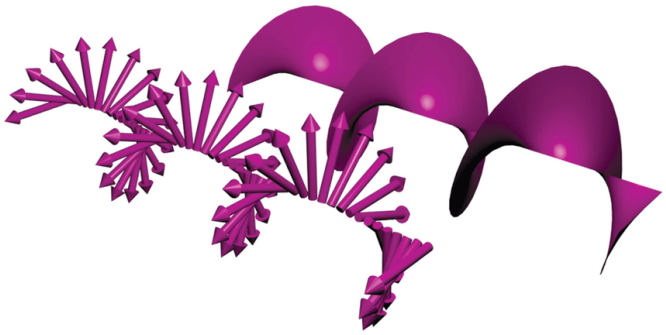

Figure 2.1: A Light Beam Carrying Spin Angular Momentum (right) and a Light Beam Orbital Angular Momentum(left)

light beam that carries only SAM and a light beam that carries OAM.

2.2 Orbital Angular Momentum of Light

Orbital angular momentum of light arises as a consequence of field spatial distribution that is, it arises as a result of the distribution of intensity and phase of the electromagnetic field. Orbital angular momentum of light has two parts – external and internal. The external OAM of light is obtained by the cross product of the position of the light beam (centre of the beam) and total linear momentum. The internal OAM is the origin dependent angular momentum that arises when a beam of light has a helical wavefront with a node at the center [8] . Such a light beam is referred to as the 'Optical Vortex'. It is a beam of light which is twisted like a corkscrew about its axis of propagation.

For the zeroth order of orbital angular momentum, the light beam is a plane wave, that is, the wavefront is a series of disconnected plane surfaces. Firstly, it is necessary to establish a paraxial wave equation to build the wave equations for higher order beams. The electromagnetic wave is a field $u(x, y, z, t)$ in space $\psi(x, y, z)$. If we consider the electromagnetic field equations to be sinusoidal, $u(x, y, z, t) = U(x, y, z, t)$ $e^{-}i\omega t$ (where $\omega = 2\pi$ f is angular frequency), then the Helmholtz equation provides a time-independent wave equation.

$$(\nabla^2 + k^2)A = 0 \tag{2.3}$$

Where, ∇ is the Laplacian operator, k is wavenumber ($k = 2\pi/\lambda$), A is normal solution constant, If we convert eqn (2.3) from cartesian coordinates to cylindrical coordinates then the equation becomes,

$$\left(\frac{1}{\psi}\right)\left(\frac{\partial}{\partial\psi}\right)\left(\psi\frac{\partial U}{\partial\psi}\right) + \left(\frac{\partial^2 U}{\partial z^2}\right) + k^2 U = 0 \tag{2.4}$$

Simplifying eqn.2.4 using $V(\psi, z) = U(\psi, z)e^{i}kz$ and the paraxial approximation $(\partial^2 V/\partial z^2) = 0$, we arrive at the paraxial wave equation.

$$\left(\frac{1}{\psi}\right)\left(\frac{\partial}{\partial\psi}\right)\left(\psi\frac{\partial U}{\partial\psi}\right) + 2ik\left(\frac{\partial V}{\partial z}\right) = 0 \tag{2.5}$$

This paraxial wave equation can be solved for the different orders of orbital angular momentum, a plane wave carries [9]. A paraxial light beam is defined as the light beam, where all the Fourier components of the optical field are well collimated and makes small angles with the axis of propagation. The amplitude of a light beam carrying OAM of $l\hbar$ has an azimuthal phase dependence of $exp(il\phi)$ Where l is the azimuthal state and ϕ is associated with its phase. This dependence arises from the analogy between Schrodinger's equation and the paraxial wave equation [7] .

The unique feature of OAM is that it can be observed across a wide range on the electromagnetic spectrum spanning across radio waves to X-rays. The most exciting aspect of photons that can carry OAM is that it enables it to trap and rotate colloid particles and even living cells, to act as a so-called 'optical spanner' [5]. That is, when angular momentum is transferred from the light beam to the matter particle, the subjected particle can be made to rotate. In 2002, a group of physicists in the University of Glasgow, were able to trap a micron sized dielectric particle in an annualar ring (a material constructed in the shape of a 2-D version of a torus) of light around the axis of the beam and were able to observe the transfer of spin and orbital angular momentum [8]. Figure (2.2) shows the simplest beam that carries an orbital angular

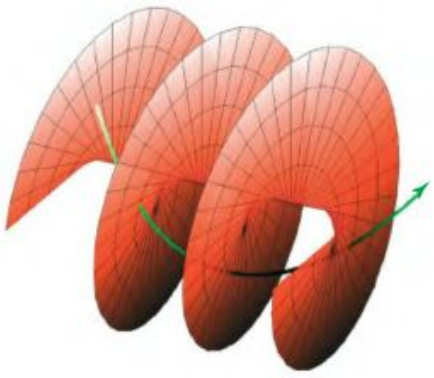

Figure 2.2: An optical vortex of order l=1 [10]

momentum, where the light beam exhibits a spiral staircase like structure with a central dark area.

To generate and observe the various properties of OAM of light, means to generate Laguerre-Gaussian beams of various orders. In order to observe and measure OAM using Fourier-Transform spectroscopy, the Laguerre-Gaussian beam is superimposed with a Gaussian beam in an interferometer.

2.3 Gaussian Beam

A Gaussian beam is a monochromatic electromagnetic radiation (waves of electromagnetic field), whose transverse electric and magnetic fields can be represented by a Gaussian function [6]. A source which emits a beam with a Gaussian profile is said to be in the fundamental transverse (TEM_{00}) mode. The geometry of a Gaussian beam wave is symmetric about the axis and varies by a radial distance about the axis [11]. When a Gaussian beam is refracted through a lens, it emerges as another Gaussian beam, this makes it the most desirable choice in beam optics experimentation. The transmitting aperture in a Gaussian beam wave is expected to be at z = 0 and the amplitude distribution of the field in this plane is Gaussian. The beam spot (w_z) refers to the radius at which the amplitude falls to 1/e of the beam's amplitude distribution [12]. When z=0, $w_{(z)} = w_{(0)}$ and $w_{(0)} = 2\sigma$ (σ - Standard deviation) as on figure 2.3.

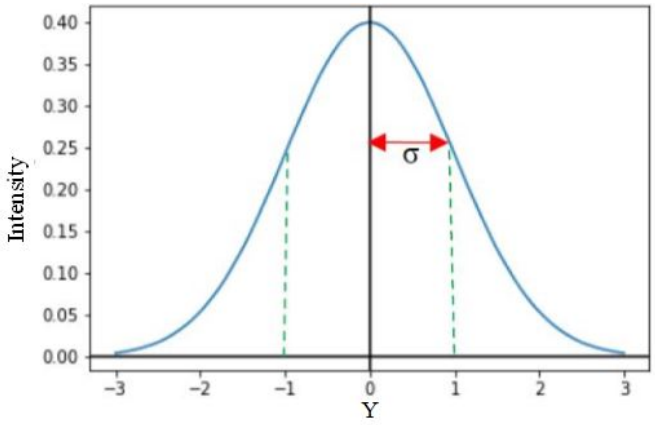

Figure 2.3: Gaussian Beam Distribution

A Gaussian beam can be represented in cylindrical coordinates as [11],
$\rho = \sqrt{x^2 + y^2}$; $\theta = tan^{-1}[\frac{y}{x}]$; z = z

$$G = u(\rho, \theta, z) = A \left[\frac{w_0}{w_{(z)}}\right] e^{-\left[\frac{\rho^2}{w^2_{(z)}}\right]} e^{i(kz-\omega t)} e^{\left[\frac{ik\rho^2}{2R(z)}\right]} \tag{2.6}$$

where, G = u(ρ, θ,z) is the wave equation of a Gaussian beam, A is the normal solution

constant, $w_{(z)}$ - Beam spot, ω is angular frequency, R(z) - radius of curvature of the wavefront. Here,

$$R(z) = z[1 + \left(\frac{z_r}{z}\right)^2] \tag{2.7}$$

Where, z_r – Rayleigh Range

$$z_r = \left[\frac{\pi w_0}{\lambda}\right] \tag{2.8}$$

In optics Rayleigh Range (refer figure 2.6) is defined as the distance measured in the

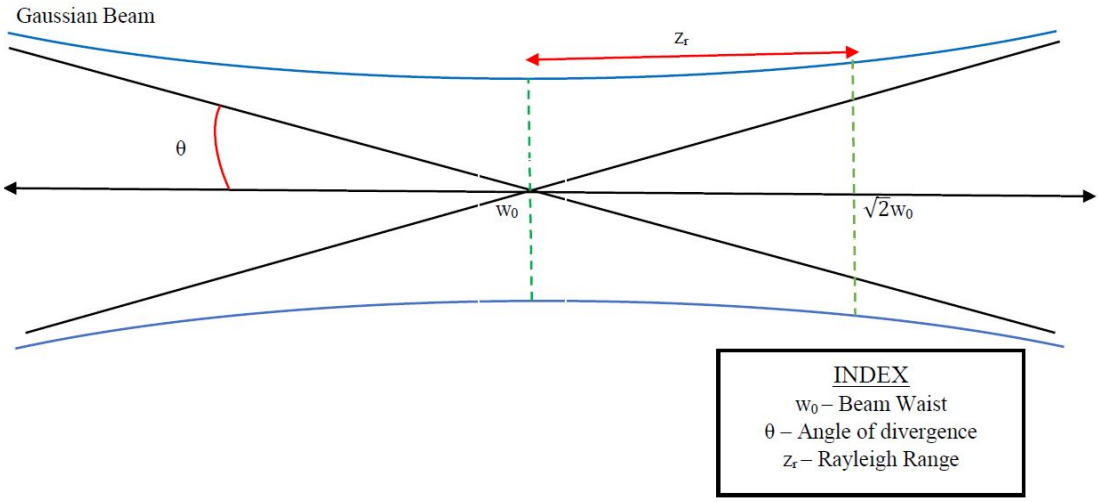

Figure 2.4: Rayleigh Range

direction of propagation of the beam between the beam waist and the point where the cross section of the beam is doubled. In eqn (2.6) the first three terms describe the amplitude of the wave and the exponents of the last three terms describe the phase of the wave. A Gaussian representation of a plane wave is chosen because a Gaussian source of distribution would remain Gaussian at every point along the propagation in the optical system even when it undergoes Fourier transformation or Fresnel Integral. For instance, the Fourier transform and the Fresnel Integral of eqn (2.6) is in the Gaussian form. This is called as the self – Fourier transform characteristic feature where the transverse intensity distribution remains constant at every point in the optical system and only the radius of the beam and the radius of curvature of the wavefront changes.

This provides mathematical tolerance while exploring the properties of OAM of light. A Gaussian beam that is focused using a lens , tends to diverge as it propagates away from the point of focus. This stands true to non – Gaussian beams, but in the case of a Gaussian beam, it differs by the trait, where the product of the width of the beam and its divergence is the smallest possible value [13]. Beam divergence is the angle between the central axis and the line that extends in the direction of the beam's radius. Beam divergence is represented as,

$$\theta \simeq \left[\frac{\lambda}{\pi w_0}\right] \tag{2.9}$$

where, θ is angle of divergence, λ is wavelength of the light, w_0 is the beam waist.

When a Gaussian beam with radius of curvature $R_{(z1)}$ is incident on lens of focal length d, then the radius of curvature $R_{(z2)}$ of the emerging beam is given by,

$$\frac{1}{R_{(z2)}} = \frac{1}{R_{(z1)}} - \frac{1}{d} \tag{2.10}$$

Here, the radius of curvature is positive when the centre of curvature is facing left. Now, the position of the minimum of the beam spot of the emergent light beam is given by,

$$z_2 = \left[\frac{R_{(z2)}}{1 + \left(\frac{R_{(z2)}}{\pi w_2^2/\lambda}\right)^2}\right] \tag{2.11}$$

Where, z_2 is the position of the minimum of the emergent beam spot, $R_{(z2)}$ is the radius of curvature of the emergent beam, w_2 is the beam waist when z=2 and λ is the wavelength. Eqn (2.11) can be simplified in using the approximation, $R_{(z2)} \ll \pi w_2^2/\lambda$ which was determined experimentally (under ordinary circumstances).

$$w_o \simeq \frac{\lambda R_{(z2)}}{\pi w_2^2} \tag{2.12}$$

Where, $w_o \simeq R_{(z2)}$ and is the beam waist under 'ordinary circumstances'.

2.4 Laguerre-Gaussian Beam

The simplest beam which can carry a well-defined orbital angular momentum is called as a *'Laguerre-Gaussian'* beam [7]. A Laguerre-Gaussian beam has a helical wavefront that is, it has rotational symmetry along its propagation axis and this characteristic is called as 'phase singularity' (optical vortex) [14]. The twist of this helical wavefront is measured by a factor called 'Topological Charge' which is an aspect that is associated with the OAM of individual photons. When macroscopic particles are subjected to these beams, they are trapped and rotated due to the transferred orbital angular momentum, in the direction of helicity of the beam. A Laguerre Gaussian beam can be generated using several optical devices, like spiral phase plate, holographic diffraction plate and birefringent liquid crystal (q-plate). These devices produce a delay in the propagation of the beam and creates a phase shift thus generating a Laguerre Gaussian beam of a specific topological charge.

A Laguerre-Gaussian beam has a phase factor that is given by $\exp(il\phi)$ where l, is the azimuthal state and ϕ is associated with its phase. When l is positive, the phase front of the light beam carrying OAM rotates clockwise and when l is negative, it rotates anti-clockwise. To derive higher order Gaussian beams it is necessary to solve the paraxial wave equations in cylindrical coordinates [11]. The wave equation of a Laguerre-Gaussian beam in cylindrical coordinates is represented as,

$$LG = \epsilon_l(\rho, \theta, z) = \left[\frac{A}{w_{(z)}}\right] \left[\frac{\sqrt{2}\rho}{w_{(2)}}\right] L_l e^{-\left[\frac{\rho^2}{w^2_{(z)}}\right]} e\left[\frac{ik\rho^2}{2R(z)}\right] e^{il\phi} \tag{2.13}$$

where, LG = $\epsilon_l(\rho, \theta, z)$ is the wave function of a Laguerre-Gaussian beam, A is normal solution constant, $w_{(z)}$ is beam spot, L^l is the Laguerre function, l is azimuthal state, ϕ is phase of the Laguerre-Gaussian beam, R(z) - radius of curvature of the wavefront. There exists a phase shift within the Laguerre-Gaussian beam due to its unique helical structure. This phase shift is represented as,

$$\Delta\phi_1 = \left[\frac{4\pi}{\lambda}\right] b(n-1) cos\left[\frac{\psi}{4}\right] \tag{2.14}$$

where, $\Delta\phi_1$ is the phase shift within the Laguerre Gaussian beam, λ is wavelength of the beam, b is thickness of the spiral phase plate, n is Refractive index of the spiral phase plate, ψ is beam position.

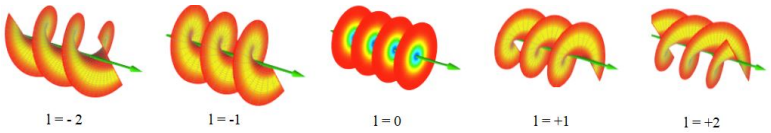

Figure 2.5: Laguerre-Gaussian Modes

Figure (2.5) shows the various phasefronts of a Laguerre-Gaussian beam for different values of l.

2.5 Methods for Generation of Orbital Angular Momentum

There are several methods used to generate 'Twisted Photons'. Some of them are as listed below.

(a) The simplest method to generate a Laguerre-Gaussian beam is to employ a spiral phase plate. A spiral phase plate is a kind of beam mode converter. In the sense, that it converts the mode of the beam that transmits through it [8]. A spiral phase plate has a constant radius but varies in thickness along its circumference. It is made of a dielectric material like Teflon whose dielectric constant (relative permittivity) is 2.1. This allows it to impose a spiral phase shift on the beam passing through it. The specific geometry shown in figure (2.6) imprints the distinctive spiral staircase like structure of a Laguerre-Gaussian beam. The spiral phase plate is built in such a way that the height between the thickest and the thinnest part of the phase plate is given by,

$$b = \left[\frac{l\lambda}{n-1}\right] \tag{2.15}$$

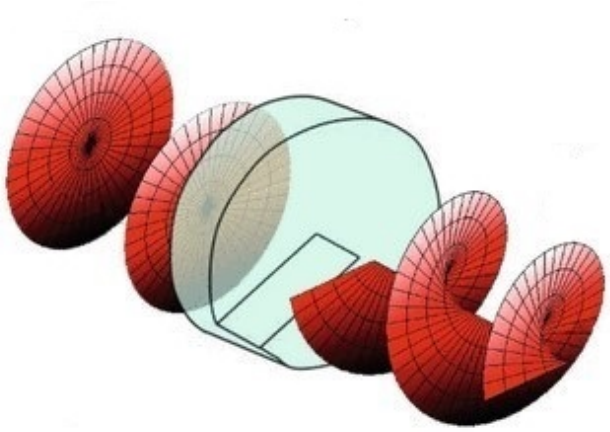

Figure 2.6: Spiral Phase Plate

Where, b is the thickness of the plate, l is the order of the Laguerre Gaussian Beam, λ is the wavelength of the light, n is the refractive index of the spiral phase plate ($n = 1.41$). The spiral phase plate delays the propagation of light differently at each point on the plate, thus causing a change in its phase. Different sizes of plates can be used to produce various orders of Laguerre Gaussian Beams.

(b) One can use a holographic diffraction plate with a pitch fork like pattern, shown in figure (2.7) to modulate the amplitude. The different colours on the holographic plate have different transmissivity.

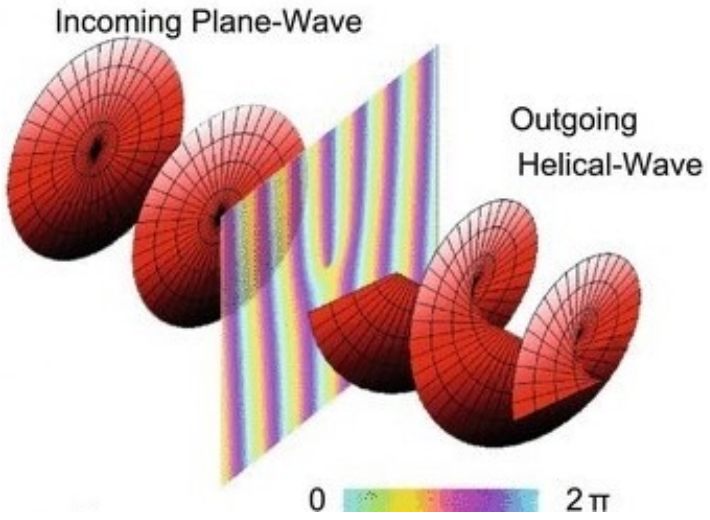

Figure 2.7: Forked Diffraction Grating

Therefore, when a Gaussian beam passes through the plate it will produce two Laguerre Gaussian beams of higher order with opposite phases. On the incidence of a Gaussian beam, parts of it that belongs to the respective azimuthal angles undergo their respective change in phase. For instance, the first-order diffracted beam will have helical phase fronts with an azimuthal index given by the number of dislocations in the pitchfork. Consequently, the wavefront of the exiting light has the helical shape of a Laguerre-Gaussian beam and a node in the centre. A Spatial Light Modulator (SLM) is a device used to impose a spatial modulation in a light beam, that is, it allows the user to impose the required change in the intensity, phase and polarization of the light beam. Used with a holographic diffraction plate, it can be used to create controlled optical traps. [15]

(c) A q-plate (refer figure 2.8) is a birefringent liquid crystal, that is, it is a liquid crystal film sandwiched between two glasses. It has a distinctive pattern as a consequence of a unique molecular alignment. When circularly polarized light transmits through a q-plate, it enforces a phase shift thus yielding an optical vortex [16]. There are two major advantages of using a q-plate to produce an optical vortex. Firstly, it does not induce any deflection on the incident light beam and secondly, it is electrically controlled, this allows the user to quickly switch polarizations. This is highly advantageous during quantum communication applications.

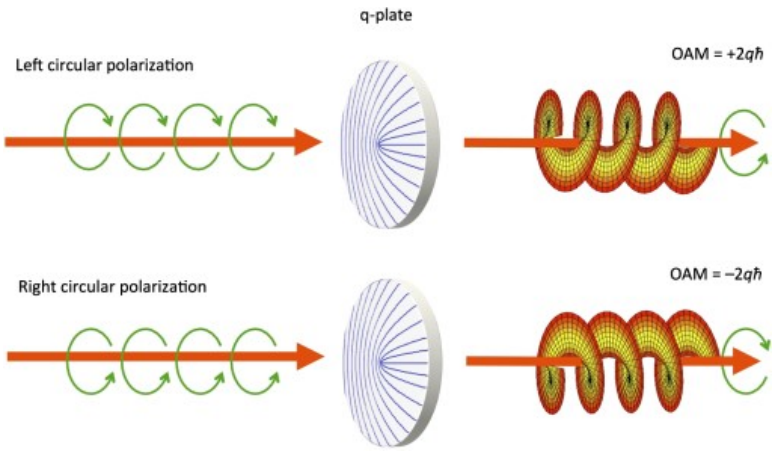

Figure 2.8: Generation of OAM of light using a q-plate from the incident circularly polarized light

(d) A cylindrical lens mode converter can be used to convert a Hermite-Gaussian beam into a Laguerre-Gaussian beam. An orthogonal set of deductions from the paraxial wave equations is called as the Hermite-Gaussian beam [17]. The

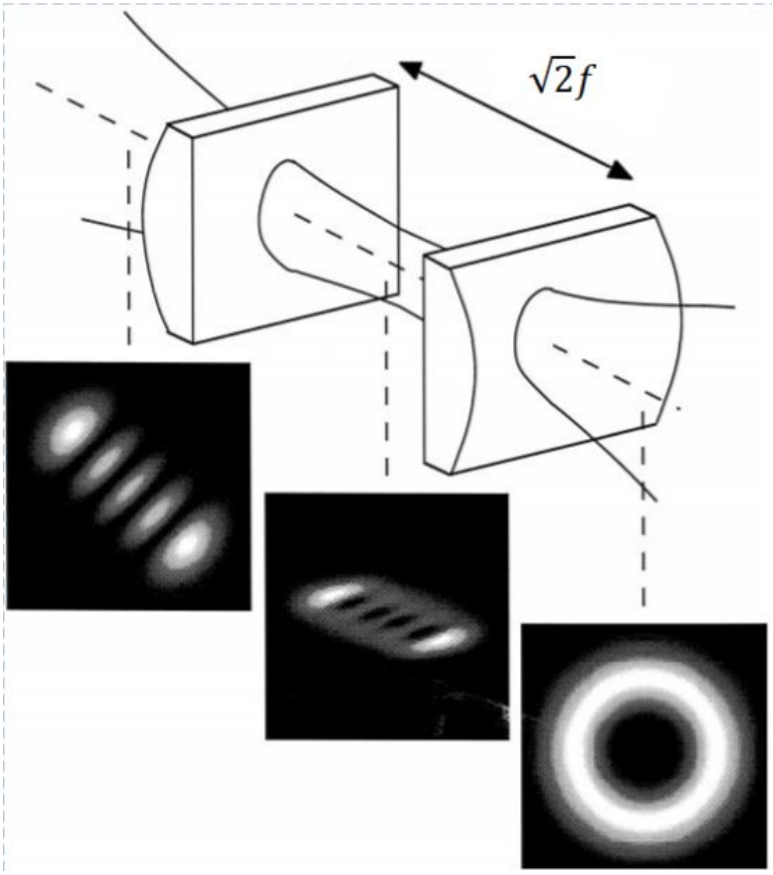

Figure 2.9: Cylindrical Lens Converter [17]

cylindrical lens converter is made up of two identical cyindrical lenses with the same focal length d, separated by a distance $\sqrt{2}d$. When a Hermite-Gaussian beam is incident at 45°, directly to the mid-point of the lens, it generates a Laguerre-Gaussian beam with the same beam waist as the Hermite-Gaussian beam. In principle this method can produce pure Laguerre-Gaussian modes better than the spiral phase plates and holographic diffraction grating.

The above methods are not compatible in experiments aiming to produce OAM of light in the UV and infrared regions of the electromagnetic spectrum. High efficiency OAM of light can be produced using an external cavity with a

quasi-matching, non-linear crystal and light carrying OAM [18]. When the crystal is aligned with the external cavity and the mode between the Gaussian pump light and the higher order Laguerre-Gaussian mode is matched highly efficient second-harmonic generation (SHG) of a light with OAM is obtained. This method has a frequency conversion efficiency of OAM of light of 10.3%.

2.6 Applications

Orbital angular momentum of light promises a revolution in optics, as it has applications in various fields like biophysics, micromechanics, communications, astrophysics, quantum information and several more.

2.6.1 Biomedicene

OAM of light allows to manipulate biological material without any contact thus becoming a topic of interest as both an enabling tool in biomedicine and a popular area of research. OAM generated in extremely small ranges whose size is smaller than human blood cells are attempting to drive micro-scale gears like biomedical devices built using nanotechnology [19].

2.6.2 Communications

It provides an additional degree of freedom in communications. This is a remarkable advantage because, up until now, information has been encoded into the two linearly independent values of the spin projection per photon. This limits the amount of information that can be transferred. But if information can be encoded in accordance with the orbital angular momentum of light, which theoretically has infinite number of probable states, it can transfer information at an extraordinary rate (about Tb/s) [5]. In addition, orbital angular momentum provides more than one bit per location on an optical disc thus propelling the efficiency of ultra-high density, optical data storage systems. It has enormous potential in quantum information processes, as it typically uses the quantum superposition of a pair of orthogonal states in a two-dimension Hilbert Space whereas OAM of light would present possibilities beyond two dimensions.

2.6.3 Astrophysics

The discovery of orbital angular momentum introduces ground-breaking variables in the field of observational astronomy specifically, to telescopes used on Earth and in observatories in space [20]. Since we obtain all the information about the various process in the Universe from spectrum of light signals, the characterization or orbital angular momentum of light or radio beams received by telescopes can provide new and perhaps crucial information about the Universe. It can also be used to overcome the Rayleigh criterium, during coronagraphic (A coronagraph is a telescopic attachment, which is used to block the direct light from a star, thus allowing the other objects around the star to be visible, which would otherwise be, engulfed in the star's glare) applications in astrophysics. Its applications in astronomy extends in interstellar and interplanetary plasma physics diagnostics, like for the detection of the rotation of a black hole [21]. Also, near by stars can be observed by converting the light obtained from it into a Laguerre-Gauss mode.

2.6.4 Quantum Cryptography

An interesting application lies in quantum cryptography. Quantum cryptography uses quantum entanglement to determine the presence of an eavesdropper. OAM of light provides an advantage in quantum cryptography by providing a high-dimensional state space, that is, each photon will now be capable of carrying larger amounts of information compared to photons with polarization alone [22].

2.6.5 Physical Chemistry

Dr. Arthur Ashkin showed that, while optical trapping takes advantage of the helical structure of the orbital angular momentum and depends on particles which have higher refractive index than its surroundings, particles with low refractive index can be employed to optically levitate a low index glass sphere against gravitational force [6]. This was achieved by using tweezers that repelled low refractive index particles from high intensity regions and attracting high refractive index particles into the trap region. The more precisely we can optically trap, rotate and manipulate particles, the more

advantage it provides in physical chemistry such as, for the precise positioning of droplets during their selective mixing [23].

2.6.6 Research in Optical

Trapping and rotating particles has been of great interest in the past decade, because this would allow one to understand the very nature of orbital angular momentum by examination of the motion of the particles rotated off-axis by an optical tweezer in a vortex light field. This would provide information which would allow one to further understand the differences between internal and external orbital angular momentum.

Chapter 3

Experimental Procedure

3.1 Fourier-Transform Spectroscopy

When two light waves with the same amplitude and wavelength, propagate in the same medium, they superimpose to form a light wave of larger or smaller amplitude. This super-position is called as *Interference* [24]. Light waves can interfere constructively or destructively. Constructive interference occurs when two light waves that are in phase with each other interfere. Destructive interference occurs when two light waves that are out of phase with each other interfere. Constructive interference produces a bright fringe on the screen, and destructive interference produces a dark fringe on the screen. For a bright fringe to appear, the path difference between the two interfering light waves must be $m\lambda$, where, m is an integer $m = 1, 2, 3..$ and λ is the wavelength of the light waves. For a dark fringe to appear, the path difference between the two interfering light waves must be $(m + 1/2)\,\lambda$.

The interferometer is an investigative device that is used in several fields of science and engineering. Their basic mechanism is to 'merge' two or more beams of light to create an interference pattern, consisting of bright and dark fringes. This interference pattern, allows the observer to determine the characteristics of the object under examination in the interferometer setup. It was Michelson and Morley who first built the device, using which they disproved the existence of a 'Lumniferous Ether' [25] atmosphere and suggested that the speed of light is invariable. The interferometer is the only device,

that allows one to make precise measurements of the light spectrum with high resolution which otherwise, would be impossible to measure. Several of the modern interferometer like LIGO (Laser Interferometer Gravitational – Wave Observatory) evolved from the Michelson interferometer.

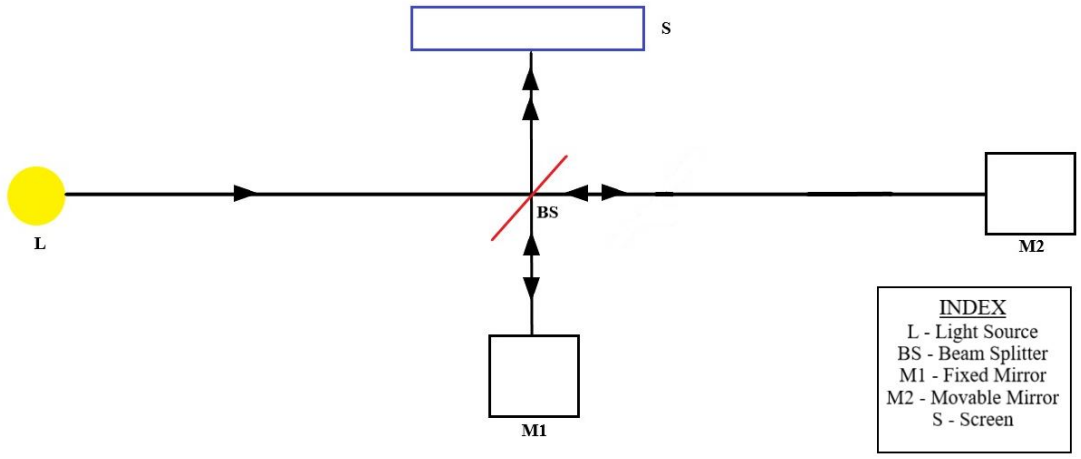

Figure 3.1: Schematic Diagram of Fourier Spectrometer

Figure(3.1) shows a basic Fourier-Transform Spectrometer that is based on the principle of Michelson Interferometer. which is capable of performing Fourier-Transform spectroscopy. This yields a resultant beam, which is produced from the interference of two or more light beams, creates an interference pattern on the camera which depends on the spectrum of the source [26]. In general, the mathematical representation of interference is based on the principle of superposition. Each of the split 'arms' of light beams, in the interferometer is an electromagnetic wave produced from the same source, either by reflection or transmission. Each of those arms is represented as follows,

$$E_1(k,x) = E_0(k).R.Te^{i2kx} \tag{3.1}$$

$$E_2(k,x) = E_0(k).R.T \tag{3.2}$$

Where, $E_1(k,x)$ and $E_2(k,x)$ represents the amplitudes of each of the electromagnetic arm, $E_0(k)$ is the amplitude of the initial wave emitted by the source, R is the reflection coefficient, T is the transmission coefficient (the product of RT represents beam splitter

coefficient), k is wave number $k = (2\pi/\lambda)$, x is the displacement of mirror M1 with respect to mirror M2, and 2x is the optical path difference between the two arms. Using the principle of superposition, the resultant amplitude of the super-imposed beam is as follows.

$$E(k,x) = E_1(k,x) + E_2(k,x) = E_0(k).R.T[1 + e^{i2kx}] \tag{3.3}$$

Eqn (3.3) shows the principle of superposition. The resultant intensity of the super-imposed beam is given as,

$$I(k,x) = |E(k,x)^2| = E_0^2(k).|R|^2.|T|^2[1 + e^{i2kx}][1 + e^{-i2kx}] \tag{3.4}$$

$$I(k,x) = g(k)(1 + cos2kx) \tag{3.5}$$

Where, $g(k) = 2E_0^2(k).|R|^2.|T|^2$ is the radiation spectrum, and $I(k,x)$ is the resultant intensity when two light waves superimpose. However, the actual spectrum of the incoming light can be much more complex and continuous. Therefore, the resultant intensity is represented as,

$$I(x) = \int_0^\infty g(k)dk + \frac{1}{2}\int_0^\infty g(k)[e^{i2kx} + e^{-i2kx}]dk \tag{3.6}$$

$$= \frac{I(0)}{2} + \frac{1}{2}\int_0^\infty g(k)e^{i2kx}dk + \frac{1}{2}\int_{-\infty}^0 g(k)e^{i2kx}dk$$

$$I(x) = \frac{I(0)}{2} + \frac{1}{2}\int_{-\infty}^\infty g(k)e^{i2kx}dk \tag{3.7}$$

Now, the interferogram power can be represented as follows.

$$w(x) = 2I(x) - I(0) = \int_{-\infty}^\infty g(k)e^{i2kx}dk \tag{3.8}$$

From eqn (3.9) it is clear that the interferogram power is the Fourier transform of the initial radiation spectrum. OAM of light is produced by placing a spiral phase plate in the interferometer and employing it to study its characteristics. To observe and investigate a Laguerre-Gaussian beam using an interferometer, it is superimposed with

a Gaussian beam. The phase shift between a Gaussian and Laguerre-Gaussian beam is,

$$\Delta\phi_2 = \left[\frac{4\pi L_l}{\lambda}\right] \tag{3.9}$$

Where, $\Delta\phi_2$ is the phase shift between a Gaussian and a Laguerre-Gaussian beam, ψ gives the coordinates for beam position, λ is the wavelength, The resultant phase shift of the super-positioned beam from Eq(2.14) and Eq(3.9) is,

$$\Delta\Phi = \left[\frac{4\pi}{\lambda}\right] b(n-1)cos\left(\frac{\psi}{4}\right) + \left[\frac{4\pi L_l}{\lambda}\right] \tag{3.10}$$

Where, $\Delta\Phi$ is the resultant phase shift, λ is the wavelength, n is the refractive index of the material of the device used to generate the Laguerre-Gaussian beam, ψ is beam position, L_l is Laguerre function.

The procedure to generate electromagnetic OAM is fairly straightforward in theory, but requires perfection as every component is particularly sensitive and therefore, the probability of misdirecting the beam is high. This involves the alignment of all the components mentioned in section 3.3. Since light in the mm wavelength region is invisible to the naked eye, the THz imaging camera is used during the setup of every component starting from the source to ensure that the alignment is according to the desired path of propagation. To produce a Laguerre-Gaussian of the first order (l=1), a spiral phase plate of radius 10 cm and thickness 10 cm is placed at close proximity infront of the stationary mirror M1, which will create a phase shift in arm $\vec{df}$. As shown in figure (3.2), the source is set to emit light with frequency 35.7 GHz and Attenutatio at 0 dB. Lense L1 is placed in front of the source at focal distance from it and focuses the Gaussian beam arm $\overrightarrow{AB}$ onto the beam splitter and lense L2 is placed in front of the camera at focal distance from it and focuses the superimposed beam arm $\overrightarrow{HI}$ onto the camera. The arm $\overrightarrow{GI}$ is the Laguerre-Gaussian beam, $\overrightarrow{AE}$ is the Gaussian beam and $\overrightarrow{DI}$ is the superpositioned beam arm. The notch on the translator is used to move mirror M2 back and forth and therefore, used to change the arm length between $\overrightarrow{DG}$ and $\overrightarrow{DE}$. This will allow the observer to see the rotational character of OAM.

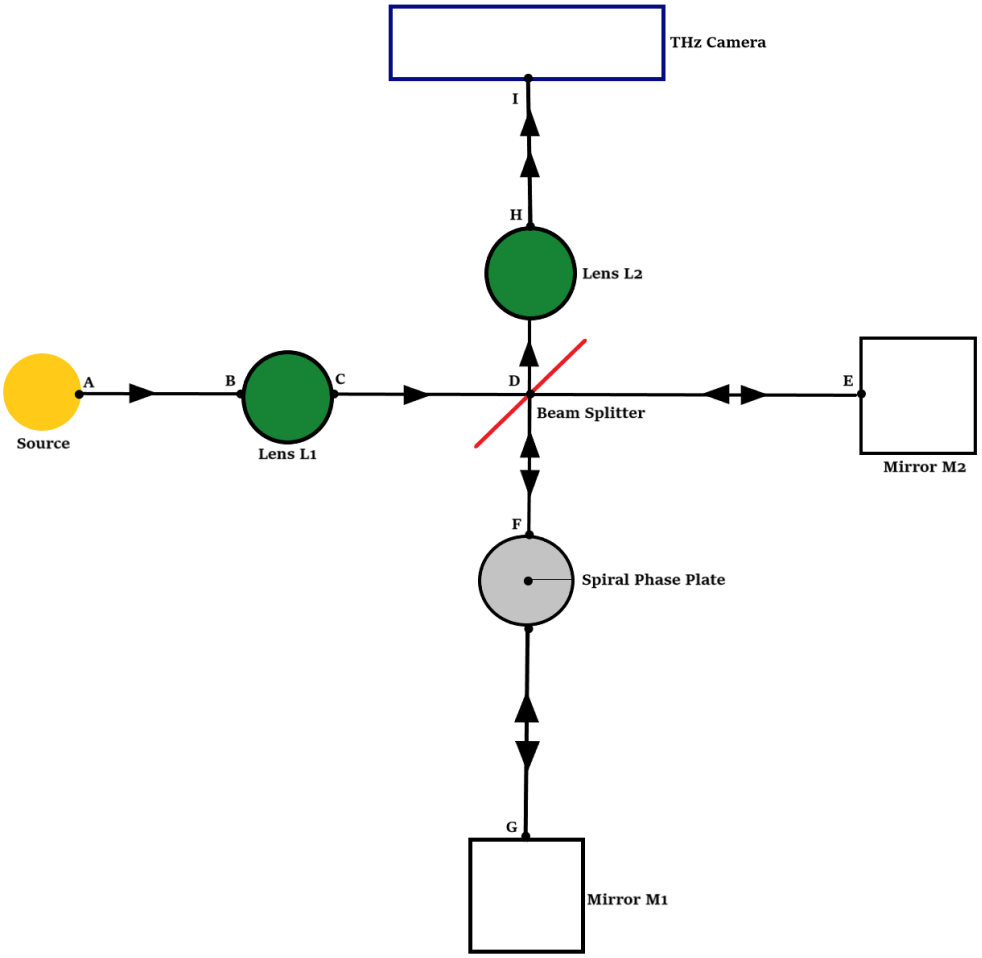

Figure 3.2: Schematic Diagram of Experimental Arrangement

3.2 Apparatus and Experimental Arrangement

OAM of light in mm wavelength region was produced using the following equipment in an Michelson interferometer setup (Using Fourier-transform spectroscopy). The experimental apparatus is setup on an optical table with microwave absorbent foam. The lenses, mirrors and the beam splitter are held into place using holders. The holders are screwed into the optical table for stability, and can be adjusted in two axis - up and down; forward and backward during alignment of the interferometer. Figure(3.3) shows the experimental setup used to obtain OAM of light. The path and direction of propagation of the Gaussian and the Laguerre-Gaussian beams by blue and orange rays respectively in figure(3.3).

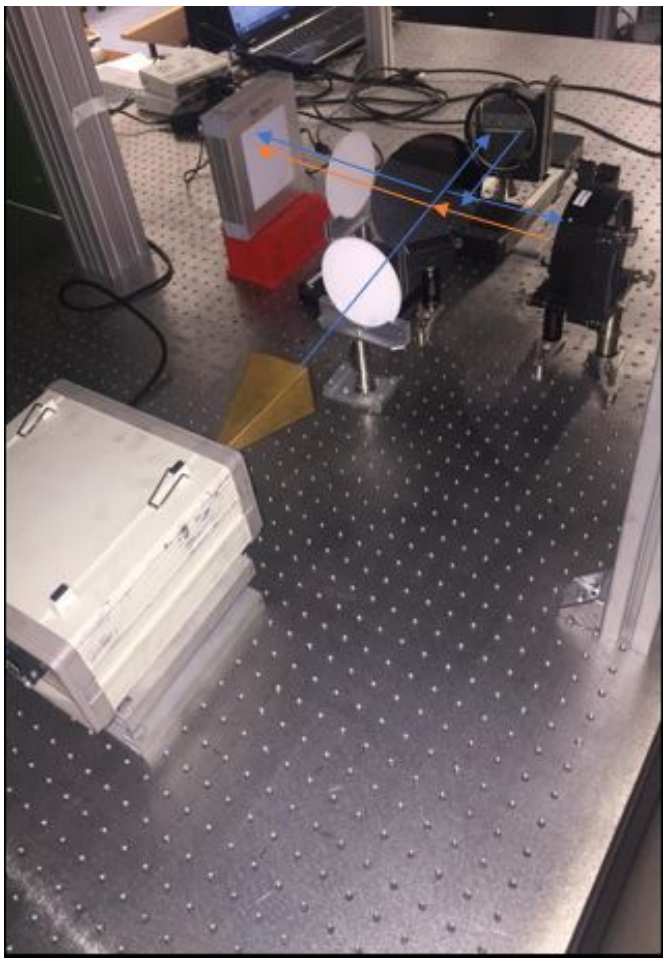

Figure 3.3: Experimental Setup

3.2.1 Source

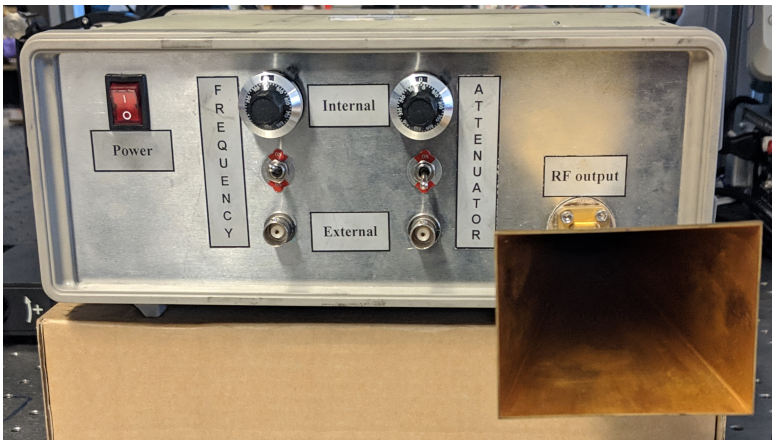

Figure 3.4: Emitter with Flared Horn Antenna

The source (refer figure 3.4) used, emits an RF output, by operating a gunn-diode. A Gunn-diode (Transfered Electron Diode(TED)) is a passive semi-conductor electronic component with two terminals and a negative resistance, which is commonly used in high frequency electronics, like electronic oscillators to produce microwaves. Its function is based on the Gunn effect discovered by J.B.Gunn in 1962 [27]. When a high voltage, which exceeds a critical value, is applied to a semi-conductor it generates a microwave power, and produces a rapidly fluctuating current. The source is modulated using two dividers - Frequency and Attenuation. This particular source has a Gunn-diode which generates voltage with frequency in the range of 13-20 GHz. A multiplier within the source increases the frequency range by a factor of 2. Then an amplifier amplifies the power and an attenuator built using waveguides limits the amount of voltage before emission. The source can emit light in the frequency range of 26.5 - 40 GHz. The light beam emitted was directed using a flared horn antenna and the frequency modulator was set to the required wavelength for the specific thickness of the spiral phase plate which was determined by eqn.

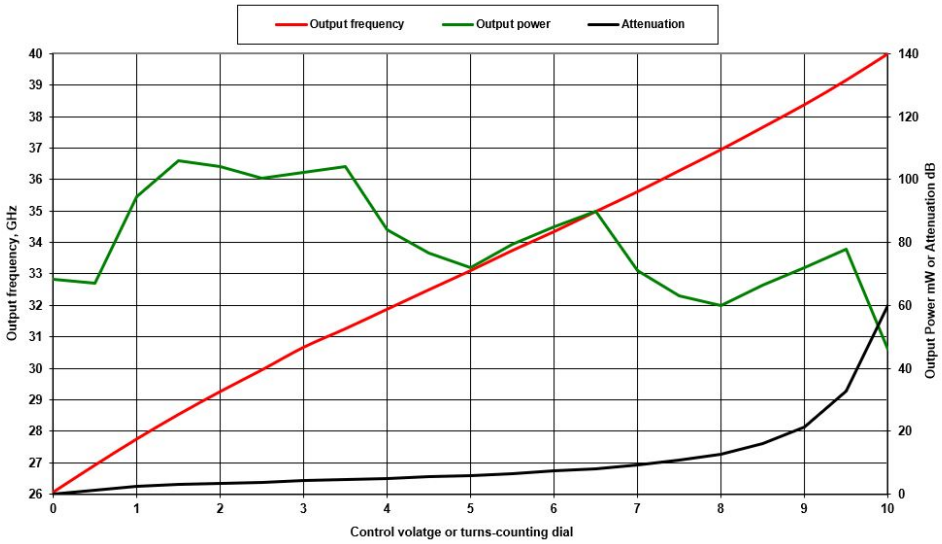

Figure 3.5: Emitter Calibration

The emitter's calibration is presented in figure (3.5). The red line represents the output frequency,the green line shows the output power and the black line indicates the amount of attenuation. The source had the following limitations - The wavelength of the light emitted could be made longer but not shorter, and it had a repetition rate of 1ms - 1KHz.

3.2.2 Lens

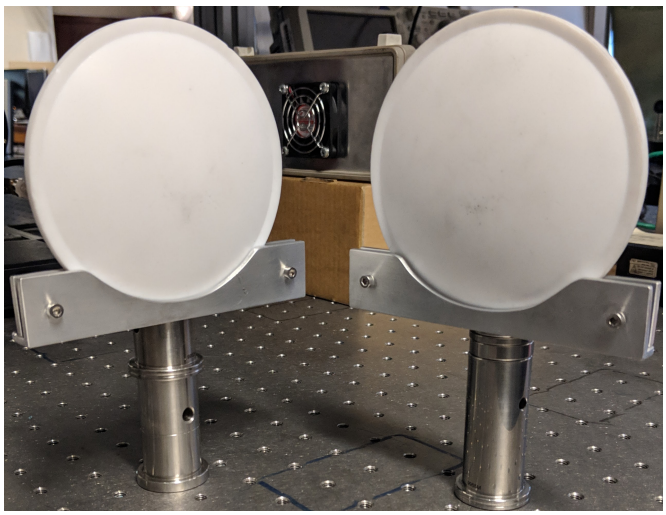

Figure 3.6: Lens Mounted on Holder

The two Teflon lenses (refer figure 3.8) used to focus the beam arms in the interferometer had an unknown focal length. This particular detail had to be determined as they were hand made. Since the lens must be placed at the focal length, which is the distance from the image sensor, at which the subject is focussed, it is necessary to determine the focal length. The images of the Gaussian beam emitted from the source were captured

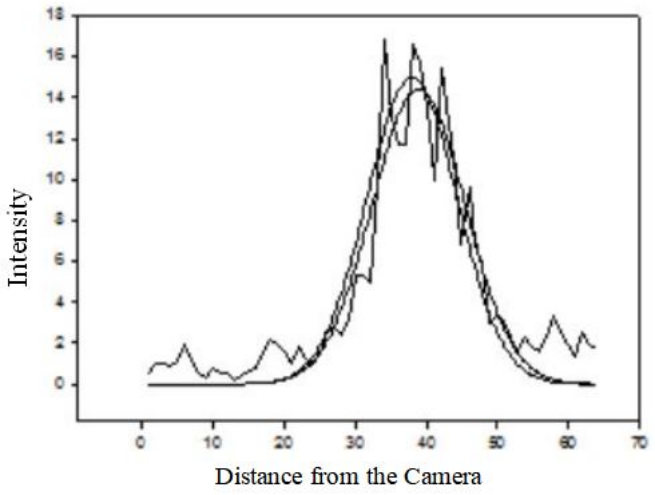

(a)

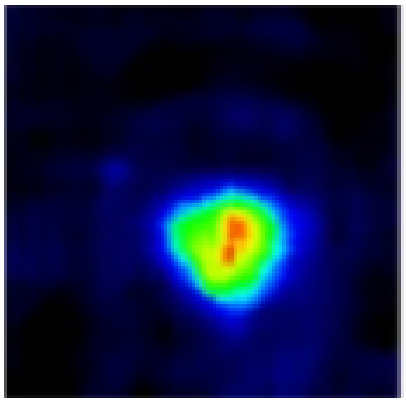

(b)

Figure 3.7: (a)Gaussian Plot of Intensity Distribution of the Image (b)Image Captured with Lens at Focal Distance from the THz Camera

at equal intervals of distance. The images were fed into SigmaPlot (SigmaPlot is a software used for data analysis and graphing) and plotted through regression analysis (refer figure (a) 3.7). The image which generated the Gaussian plot (refer figure (b) 3.7), that had the highest intensity and the smallest width was determined to be captured at the focal length of the lens. The focal length for the lens was determined to be 20

cm. In the interferometer setup, two lenses are placed at precise focal distances, one to focus the Gaussian beam emitted by the source onto the beam splitter and the other to foucs the superpositioned beam onto the THz camera.

3.2.3 Beam Splitter

A beam splitter (refer figure 3.8), is an optical device which is used to split the incident light beam into two parts. The beam splitter used in the experiment, to split mm-waves has a transmission to reflection ratio of 50:50, therefore, it splits the incident beam into equal halves. The beam splitter, used for the experiment is 10 cm in diameter and is made of Silicon. In order to ensure an equal split of the incident beam it is placed at a 45° angle to the plane of the propagating wavefront, leading to a 90° deflection and transmission in two directions.

Figure 3.8: Beam Splitter

3.2.4 Spiral Phase Plate

Spiral phase plate or a tweezer shown in figure (3.9) is an optical device which differs consistently in radius but has a fixed circumference. The spiral phase plate used is made of Teflon which has a refractive index of 1.42. Each spiral phase plate requires a specific frequency of light that needs to be emitted in order to produce the required order of Laguerre-Gaussian beam. The thickness of the tweezer used to generate a Lagurre-Gaussian beam of the first order is 10cm with a radius of 5cm. These spiral

phase plates fit perfectly into a standard mirror holder and were screwed down into the optical table.

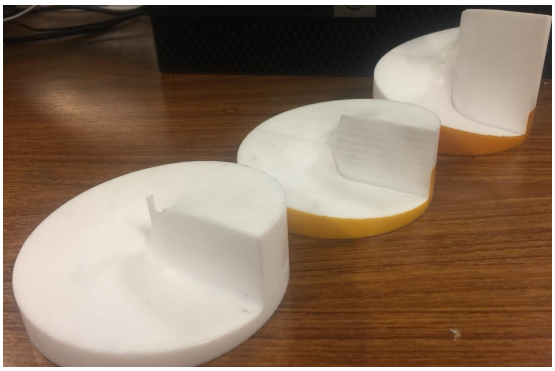

Figure 3.9: Spiral Phase Plates of Varying Thicknesses

3.2.5 Mirrors

Figure (3.10) shows the two identical mirrors of diameter 10 cm are used in the interferometer setup. Mirror M1 is stationary and mirror M2 is movable on a micro control translator. The mirrors are placed perpendicular to each other. The micro control translator is used to move mirror M2, changing the beam's arm length between the two mirrors. The micro control translator (refer figure 3.10 (b)) is manufactured by Newport Corporation(Model:UE34CC) provides steady and controlled movement, using the notch provided. This allows the observer to witness the rotational symmetry trait of OAM.

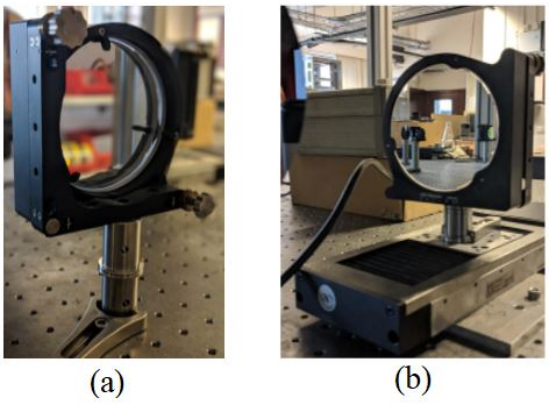

Figure 3.10: (a) Mirror M1 (b) Mirror M2

3.2.6 THz Camera

The part of the electromagnetic wave that has been the least explored is the region between radio waves and infrared light. It was a team from University of Wuppertal which utilized the less used terahertz band which provided the means to accesses these regions of the electromagnetic spectrum. They developed a CMOS camera which is sensitive to terahertz frequencies.This became the model over which the currently used terahertz camera was built. Figure (3.11) shows the terahertz imaging camera (Model number: Tera-4096) used to capture the images was manufactured by Terasense, and is a sub-THz imaging sensor which operates in room temperature. The sensitivity band of the camera (refer figure 3.11)ranges approximately 50-700 GHz. The camera is sensitive to polarization and the preferred direction of polarization is parallel and upwards on the plane of the camera. It has 4096 pixels and has a Noise Equivalent Power (NEP)

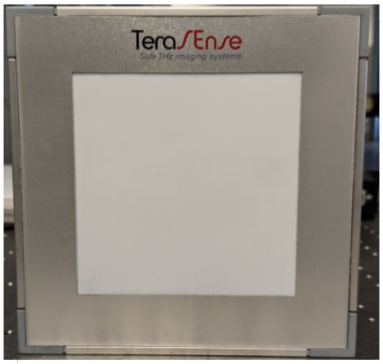

Figure 3.11: THz Camera

of 1 nW/$\sqrt{Hz}$. NEP is the sensitivity factor of a camera. It is determined by the ratio of signal to noise level. In this case the signal and noise level are equal. It is 4096 pixels with each pixel being 1.5 X 1.5 mm. The camera has a pixel pitch of 1.5 mm and a responsivity of 50 kV/W. Pixel pitch denotes the density of pixels on the camera. Smaller the pixel pitch higher will be the resolution.

3.3 Observation

A live view from the camera was used to observe the images. It shows the intensity distributed across the pixels on the camera. In order to obtain images with clarity, the camera feed is set to specific image properties such as exposure and white balance. The Gaussian beam was first captured without the interferometer in a setup as shown in figure(3.12)

The emitter, lens and the THz camera are placed, linearly on the optical table. The

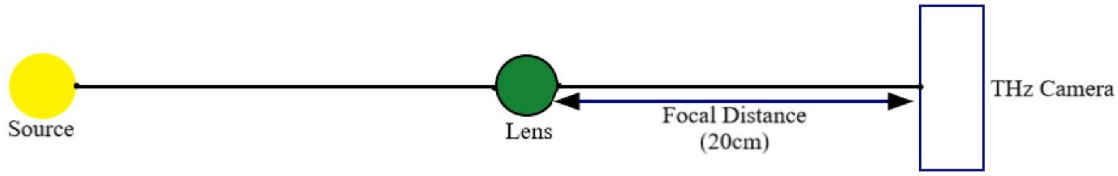

Figure 3.12: Schematic Diagram of Experimental Setup for Direct Image of Gaussian Beam

lens is placed at focal distance from the camera, to focus the beam onto it. To verify and to manipulate OAM of light, every step of the experiment was simulated in a Python environment. The intensity of Gaussian beam wave equation that is coded in Python is as follows,

$$I_G \propto e^{(\sqrt{x^2+y^2})} \tag{3.11}$$

Where, I is the intensity of the Gaussian beam, x and y are positions in Cartesian coordinates. The image of the Gaussian beam which was received from the setup shown in figure (3.12) was a fairly circular spot with its intensity decreasing outward from the centre. The Gaussian beam image obtained from equation coded is similar to image observed via experimental procedure.

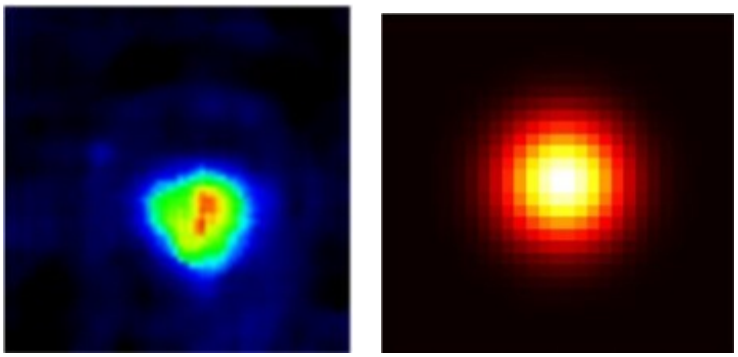

(a) (b)

Figure 3.13: (a) Direct Image of a Gaussian Beam from Experimental Method(b) Direct Image of a Gaussian Beam Generated in a Python Environment

A direct image of the Laguerre-Gaussian beam is obtained by aligning the emitter, spiral phase plate, lens and the THz camera linearly on the optical table as shown in figure (3.14). The intensity of Laguerre-Gaussian beam wave equation that is coded in

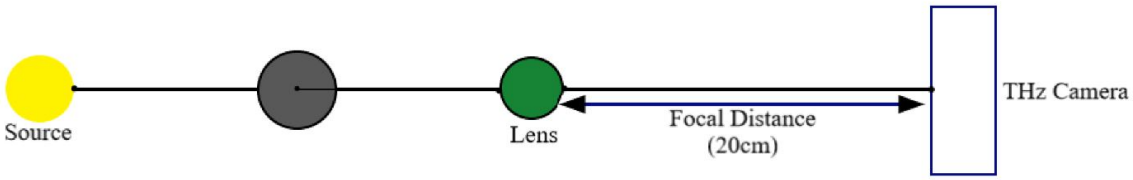

Figure 3.14: Schematic Diagram of Experimental Setup for Direct Image of Laguerre-Gaussian Beam

Python is as follows,

$$I_{LG} \propto \sqrt{(x^2+y^2)^l} e^{\left(\sqrt{x^2+y^2}\right)} \tag{3.12}$$

Where, I is the intensity of the Laguerre-Gaussian beam, l is the azimuthal state, x and y are positions in Cartesian coordinates. The direct image of a Laguerre-Gaussian beam (as shown in figure 3.15) obtained from the experimental setup shown in figure (3.14) appears in the shape of a vague annular ring. The varying intensities along the annular ring is due to varying thicknesses of the spiral phase plate. A similar annular ring is obtained in the Python environment, where the intensity distribution is plotted. To produce interference The interferometer is setup on the optical table, using holders, with the emitter set at frequency 35.7 GHz and attenuation at 9.2 dB as shown in figure

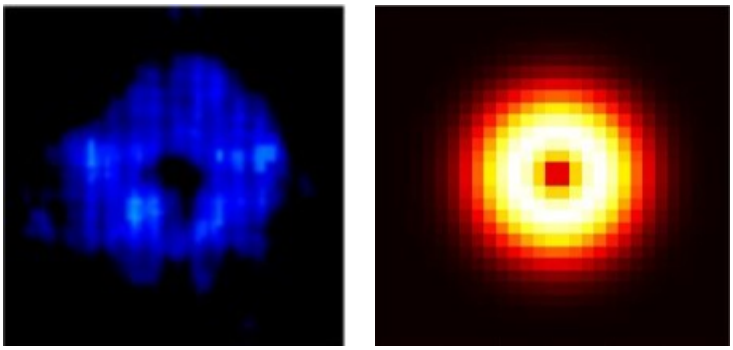

(a) (b)

Figure 3.15: (a) Direct Image of a Laguerre-Gaussian Beam from Experimental Method(b) Direct Image of a Laguerre-Gaussian Beam Generated in a Python Environment

(3.2). A spiral phase plate of thickness 10cm is placed in the arm $\overrightarrow{DG}$. The image of the interference of a Gaussian and a Laguerre-Gaussian beam is captured from the live feed received on the terasense application. The interference is also generated in a Python environment using the total phase shift give by,

$$\Delta\Phi = I_G^2 + I_{LG}^2 + 2I_G I_{LG}[1 + \cos(\Delta\phi_1)] \tag{3.13}$$

Where, $\Delta\Phi$ is the resultant phase shift of the super-positioned beam, I_G is the intensity of the Gaussian beam, I_{LG} is the Intensity of the Laguerre-Gaussian beam,$\Delta\phi_1$ is the phase shift within the Laguerre-Gaussian beam. The image of interference obtained resembles a bean with a tail. The intensity distribution of the total phase shift plotted in a Python environment generated a similar result. In order to observe the rotational feature of the helical structure of a Laguerre-Gaussian beam carrying orbital angular momentum of the first order, the micro control translator is moved in equal distances given by,

$$\sigma = rms = \frac{1}{\sqrt{2}} \tag{3.14}$$

$$\Delta x = \Delta y = \frac{1}{3\sqrt{2}} \approx 0.2cm \tag{3.15}$$

Where, σ is root mean square.

Images of interference were captured by changing the path length between mirror M1 and mirror M2 by moving the mirror M2 at steps of 0.2cm in one direction. The image

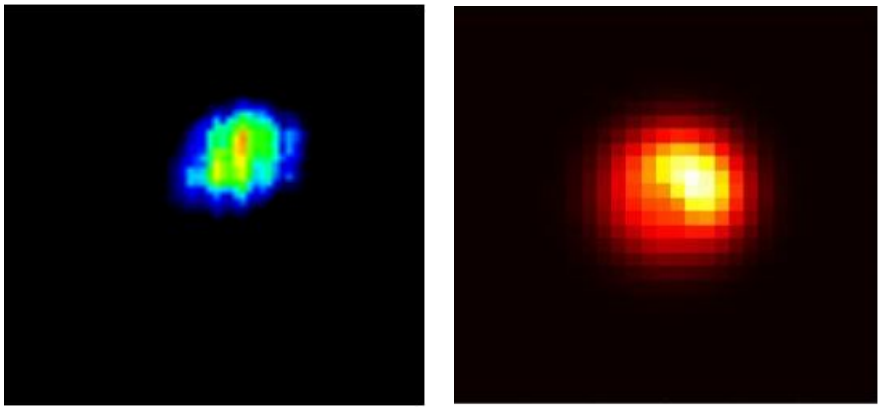

(a) (b)

Figure 3.16: (a) Direct Image of a Laguerre-Gaussian Beam from Experimental Method(b) Direct Image of a Laguerre-Gaussian Beam Generated in a Python Environment

which resembled a bean with a tail was observed to rotate along a circumference.

The sequence of images, displaying the rotational characteristic of a helical beam obtained by changing the path length between the two mirrors in the setup (refer figure 3.2) is shown in comparison to the same effect generated in a Python environment by changing the path lengths between the Gaussian and the Laguerre-Gaussian beams. In order to understand the different beams that were generated and verify the observed characteristics of OAM, the entire experiment was simulated in a Python environment. The Gaussian and a Laguerre-Gaussian beams were obtained using the code in figure(A.2) and figure(A.3). Column (A) shows images obtained in the Python environment and Column (B) shows the images obtained from the experimental procedure. Both the columns depict the rotational characteristic of the helical structure of OAM of light looping about the propogation axis.

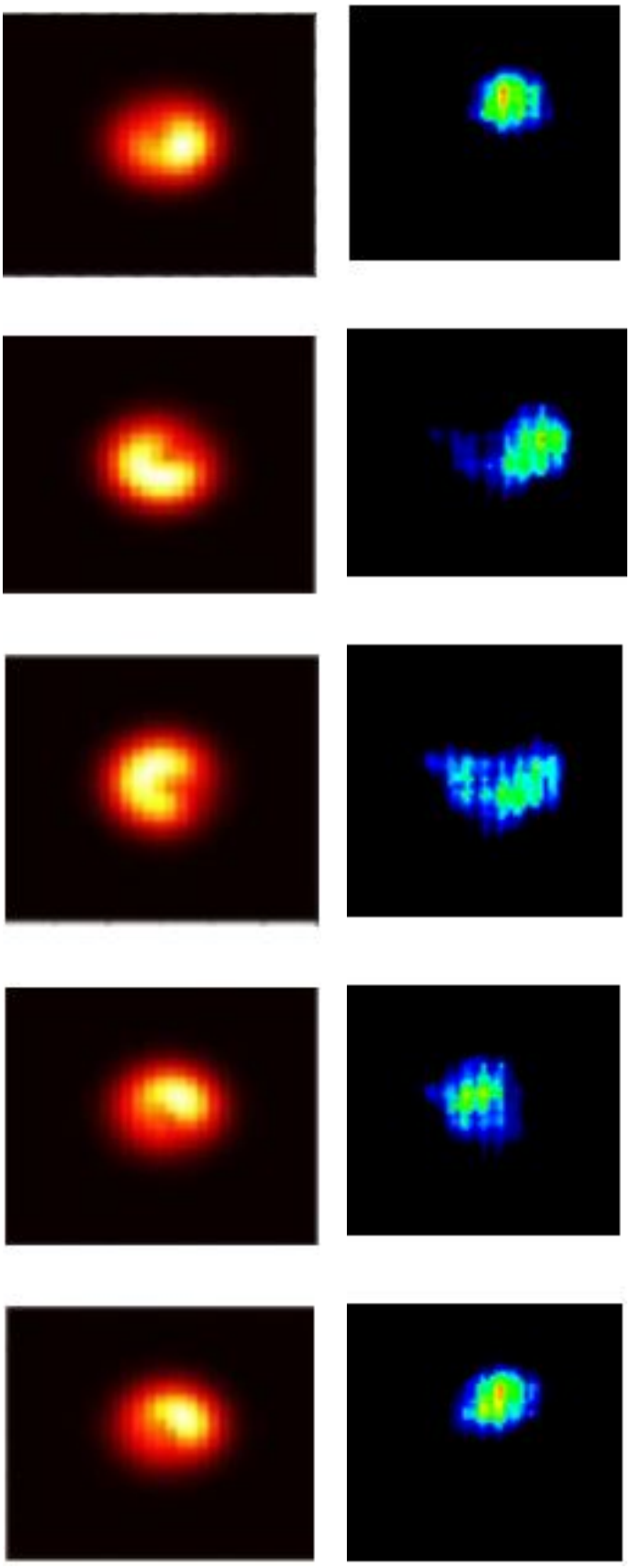

(a) (b)

Figure 3.17: Interference Image Captured by Sequential Change of Path Difference Between the Gaussian and the Laguerre-Gaussian Beams in (A) a Python Environment (B) through Experimental Procedure

Chapter 4

Conclusion

Since, OAM is a recently developing subject, its knowledge lies among very few papers. These papers were studied, composed and summarized into simple terms, which is written in a logical order for easier understanding. An interferometer based on Fourier transform spectroscopy was aligned with a spiral phase plate (optical tweezer) of thickness 10cm. OAM of the first order was generated in the mm wavelength region ($f = 35.7Ghz$).The Gaussian and the Laguerre-Gaussian beams were superimposed, and the resultant image was observed using a THz imaging sensor. The images obtained, were also theoretically generated in a python environment and the images obtained were confirmed to be similar with the experimental results, taking into consideration misalignments due to the high sensitivity of the interferometer and parallax errors that accompany an experimental setup which is aligned by hand. Several of the mistakes that occurred during the experimental setup and the simulation in the Python environment occurred due to lack of attention to the detail in the characteristics of OAM. A lot of mistakes could have been avoided and precious time could have been saved, if its theory was first understood before jumping head first into the project. OAM of light has much to be explored. The generation of OAM in the mm wavelength region, in higher-orders using emitters with higher powers has the potential of moving objects made of metal. Further theoretical understanding of its characteristics and experimental observations are necessary to truly realize the outstanding applications they promise.

Appendix A

Simulation of Experimental Procedure

Figure(A.1) shows the code that was used for initializing the necessary variables. For ease of coding, the beam's wave equations are coded in Cartesian coordinates and the number of parameters used to describe them are constricted to the shape and position of the beam. Figure (A.2) shows the code used to generate the Gaussian beam in a

```
import numpy #Import numerical python library
import matplotlib.pyplot as plt #Import library for plotting
import math
from scipy import special
w=1 #peak to peak diameter of the doughnut
x= numpy.linspace(-3,3,30) #Makes an array of x coordinate
y= numpy.linspace(-3,3,30) #Makes an array of y coordinate
shape = 30 #Defines the number of elements in your array
lamda=8.4
l=1
n=1.42
d=10
```

Figure A.1: Code for Assigning Variables

Python environment is given in figure Figure (A.3) shows the code used to generate the

```
#-------------------------GAUSSIAN----------------------------------------

def G(x,y):
    return numpy.exp(-(x**2+y**2))
G_array=[G(elemx,elemy)for elemx in x for elemy in y] #Solves the function for
# x and y elements and it is of type'list'
G_array=numpy.array(G_array) #Converts the 'list' to 'array' of 900 elements
G_array=G_array.reshape (shape,shape)#Converts the column into a 30X30 matrix
plt.pcolormesh(x,y,G_array,cmap='hot')#Function for plotting a distribution
plt.show()
```

Figure A.2: Code Used to Generate the Intensity Distribution of a Gaussian Beam

Laguerre-Gaussian beam in a Python environment is given in figure Figure (A.4) shows

```
#------------------------LAGUERE GAUSSIAN-------------------------------------
def LG(x,y): #The function describes the LG mode
    return  ((x**2+y**2)**0.5)**l *numpy.exp(-(x**2+y**2))
LG_array=[LG(elemx,elemy)for elemx in x for elemy in y]#Solves the function for
#x and y elements and it is of type'list'
LG_array=numpy.array(LG_array)#Converts the 'list' to 'array'of 900 elements
LG_array=LG_array.reshape (shape,shape)#Converts the column into a 30X30 matrix
plt.pcolormesh(x,y,LG_array,cmap='hot')#Function for plotting a distribution
plt.show()
```

Figure A.3: Code Used to Generate the Intensity Distribution of a Laguerre-Gaussian Beam

the code used to simulate the interference image obtained from the experimental setup, where the image is generated with respect to the total phase shift the resultant beam carries.

```
#----------------------INTERFERENCE-----------------------------------------
def dphi(x,y,L):
    return ((4*numpy.pi/lamda) *d* (n-1)) *
numpy.cos(numpy.pi/4+numpy.arctan2(y,x)/4) + (4 * numpy.pi * L / lamda )
def final(x,y,L):
   return LG(x,y)**2+G(x,y)**2 +2*LG(x,y)*G(x,y)*(1+numpy.cos(dphi(x,y,L)))
L=1
print (dphi(x,y,L))
final=[final(elemx,elemy,L)for elemx in x for elemy in y]
#Solves the function for x and y elements and it is of type'list'
final=numpy.array(final)#Converts the 'list' to 'array' of 900 elements
final=final.reshape (shape,shape)#Converts the column into a 30X30 matrix
plt.pcolormesh(x,y,final,cmap='PuBu_r')#Function for plotting a distribution
plt.colorbar()

plt.show() #Function that seperates and displays the three different plots
```

Figure A.4: Code Used to Generate the Intensity Distribution of the Interference Image Generated by the Superposition of a Gaussian and a Laguerre-Gaussian Beam

Bibliography

[1] Thomas F. Maxwell, James C.; Torrance. A Dynamical Theory of the Electromagnetic Field. *Philos. Trans. R. Soc. London*, 1865.

[2] J.H Poynting. The Wave Motion o f a Revolving Shaft, and a Suggestion as to the Angular Momentum in a Beam of Circularly Polarised Light. In *Proc. R. Soc. London. Ser. A, Contain. Pap. a Math. Phys. Character*, number 2, pages 560–567, 1909.

[3] Albert Einstien. The quantum theory of radiation damping. *Math. Proc. Cambridge Philos. Soc.*, 37(3):301–316, 1941.

[4] Arthur H. Compton. A Quantum Theory of the Scattering of X-rays by Light Elements. *Phys. Rev.*, 21(5):483–502, 1923.

[5] Richard A. Beth. Mechanical detection and measurement of the angular momentum of light. *Phys. Rev.*, 50(2), 1936.

[6] A. Ashkin. Acceleration and Trapping of Particles by Radiation Pressure. *Phys. Rev. Lett.*, 11(2), 1970.

[7] L. Allen, M. W. Beijersbergen, R. J.C. Spreeuw, and J. P. Woerdman. Orbital angular momentum of light and the transformation of Laguerre-Gaussian laser modes. *Phys. Rev. A*, 45(11):8185–8189, 1992.

[8] A. T. O'Neil, I. MacVicar, L Allen, and M J Padgett. Intrinsic and Extrinsic Nature of the Orbital Angular Momentum of a Light Beam. *Phys. Rev. Lett.*, 88(5):053601, jan 2002.

[9] Timothy Doster and Abbie T. Watnik. Laguerre–Gauss and Bessel–Gauss beams propagation through turbulence: analysis of channel efficiency. *Appl. Opt.*, 55(36):10239, 2016.

[10] Juan P. Torres and Lluis Torner. *Twisted Photons: Applications of Light with Orbital Angular Momentum*. 2011.

[11] Enrique J. Galvez. Gaussian beams in the optics course. *Am. J. Phys.*, 74(4):355–361, 2006.

[12] Ronald L. Phillips Larry C. Andrews. *Laser Beam Propagation through Random Media, Second Edition*. 2005.

[13] Malvin Carl Teich Bahaa E. A. Saleh. *Fundamentals of Photonics*. Wiley, 2007.

[14] Sharon A. Kennedy, Matthew J. Szabo, Hilary Teslow, James Z. Porterfield, and E. R.I. Abraham. Creation of Laguerre-Gaussian laser modes using diffractive optics. *Phys. Rev. A - At. Mol. Opt. Phys.*, 66(4):438011–438015, 2002.

[15] Daryl Preece. *Novel Uses of Spatial Light Modulators in Optical Tweezers*. PhD thesis, University of Glasgow, 2011.

[16] Lorenzo Marrucci, Lorenzo Marrucci, Napoli Federico, and Dipartimento Fisica. The q-plate and its future. *J. Nanophotonics*, 7, 2013.

[17] J. Courtial and M. J. Padgett. Performance of a cylindrical lens mode converter for producing Laguerre-Gaussian laser modes. *Opt. Commun.*, 159(1-3):13–18, 1999.

[18] Zhi-Yuan Zhou, Yan Li, Dong-Sheng Ding, Yun-Kun Jiang, Wei Zhang, Shuai Shi, Bao-Sen Shi, and Guang-Can Guo. High efficiency SHG of orbital angular momentum light in an external cavity. *Opt. Express*, 22(19):23673—-23678, 2014.

[19] Adam Mann. Core Concept: "Twisted" light beams promise an optical revolution. *Proc. Natl. Acad. Sci.*, 115(22):5621–5623, 2018.

[20] Daisuke Akamatsu and Mikio Kozuma. Coherent transfer of orbital angular momentum from an atomic system to a light field. *Phys. Rev. A - At. Mol. Opt. Phys.*, 67(2):8, 2003.

[21] Martin Harwit. Photon Orbital Angular Momentum in Astrophysics. *Astrophys. J.*, 597(2):1266–1270, 2003.

[22] A Padgett, M. Yao. Orbital Angular Momentum: origins, behavior and applications. *Adv. opt. Phot.*, 3(2):161–204, 2011.

[23] A. Jones, P. Zemanek. Light at Work: The use of optical forces for paricle manipulation. *Electrophoresis*, 29:4813–51, 2009.

[24] Max; Born and Emil Wolf. *Principles of Optics: Electromagnetic Theory of Propagation, Interference and Diffraction of Light.* Pergamon Press, sixth edit edition, 1987.

[25] Albert A. Michelson, E. Morely. On the Relative Motion of the Earth and the Luminiferous Ether. *Am. J. Sci.*, (203), 1887.

[26] Graham Smith, Terry King, and Dan Wilkins. *Optics and Photonics.* Wiley, second edition, 2007.

[27] Zaffrul Zulkarnain Aziz Masuaud, Mohd Azlishah Othman, Nadhirah Ali, Hamzah Asyrani Sulaiman, and Mohamad Zoinol Abidin Abd Aziz. An analysis of D-band gunn diode for millimeter wave application. *ARPN J. Eng. Appl. Sci.*, 10(2):661–665, 2015.